H I OBSERVATIONS OF THE LOCAL GROUP DWARF WLM

DALE C. JACKSON, EVAN D. SKILLMAN, AND JOHN M. CANNON[1]

Department of Astronomy, University of Minnesota, 116 Church Street SE, Minneapolis, MN 55455;
djackson@astro.umn.edu, skillman@astro.umn.edu, cannon@astro.umn.edu

AND

STÉPHANIE CÔTÉ

Herzberg Institute of Astrophysics, National Research Council of Canada, 5071 West Saanich Road,
Victoria, BC V9E 2E7, Canada; stephanie.cote@nrc.gc.ca

ABSTRACT

We present Australia Telescope Compact Array mosaic H I imaging of the Local Group dwarf irregular galaxy WLM. We find an integrated flux of 149 Jy km s^{-1} and a total H I mass of $(3.2 \pm 0.3) \times 10^7 \, M_\odot$. The major axis of the H I is aligned with the stellar component of the galaxy. The overall H I distribution is relatively smooth at our resolution and has a double-peaked central core. One of these peaks is aligned with a region found to have extinction that is internal to WLM, and we take this as possible evidence of a large molecular gas complex in the southern half of the galaxy. The other H I peak is in close proximity to the brightest H II regions. WLM's overall velocity field is consistent with rigid-body rotation. A rotation curve is derived, and we find a total dynamical mass of $(3.00 \pm 0.80) \times 10^8 \, M_\odot$. We also performed a wide-field search, $38'$ in radius, for H I companions or evidence of recent interactions (e.g., tidal tails) and found no detections to an H I mass limit of $M_{\mathrm{H\,I}} > 8.4 \times 10^5 \, M_\odot$.

Key words: galaxies: dwarf — galaxies: individual (WLM) — galaxies: irregular — Local Group

1. INTRODUCTION

The WLM dwarf irregular galaxy (DDO 221, UGCA 444) is a member of the Local Group. Its basic properties are listed in Table 1. Since its discovery (Wolf 1910; Melotte 1926), there have been numerous studies of its photometric proper-ties, stellar populations, star formation history, and chemical abundances (van den Bergh 2000). Unfortunately, other than observations of H II regions (Hodge & Miller 1995), an un-successful search for CO (Taylor & Klein 2001), and studies of its most basic infrared (Melisse & Israel 1994) and radio (Huchtmeier et al. 1981; Huchtmeier & Richter 1986) prop-erties, little has been done to study its interstellar medium.

Understanding the neutral hydrogen content in WLM is particularly important for a number of reasons. The first is that at a distance of 0.95 ± 0.04 Mpc (Dolphin 2000), a detailed study of the stellar populations of WLM is within reach. This allows us to directly observe the interplay between the stars and the interstellar medium (ISM). From a phenomenological point of view, it only makes sense that we have as detailed an understanding as is possible of the most nearby galaxies to support assumptions about galaxies whose properties are not as easily resolvable. Also, WLM is one of only a handful of ir-regular galaxies that are close enough for detailed analyses and that are also relatively isolated in space. This provides us with an excellent opportunity to examine the evolution of a galaxy without evidence of recent interaction with its neighbors.

One unique aspect of WLM is a discrepancy between H II region and Population II stellar abundances. A recent study by Venn et al. (2003) found the oxygen abundance of a WLM supergiant to be much higher than the nebular abundance of the sampled H II regions. This is puzzling, since the young

stars form from the galaxy's ISM and thus should not have a higher metallicity than the gas. Although a larger stellar sample size is clearly needed to determine if the abundance offset is real, a possible explanation is that high-metallicity stars became associated with, but did not form from, the low-metallicity gas through a merger. If, in fact, a recent merger did occur, it may be observable through H I observations.

By studying the ISM, and particularly the neutral hydrogen, of dwarf galaxies we can extract information about recent star formation events, mergers, and the galaxy's ability to form stars in the future. Additionally, we can derive a rotation curve for the galaxy and determine its dynamical mass. As WLM is close enough to resolve into stars, we can compare the derived mass-to-light ratio to what is expected from its stellar popu-lation. Since H I observations are the most direct method of observing the large-scale motions of a galaxy's ISM, contin-ued progress with the study of dark matter relies on high spatial and spectral resolution observations to study the kin-ematics of the ISM in these galaxies.

In this paper we present the highest spectral and spatial resolution study of the H I in WLM to date. Section 2 de-scribes the ATCA mosaic observations and reduction of the data. In § 3 we analyze the total H I flux and compare its distribution to that of the optical. The H I position-velocity diagrams and WLM's derived rotation curve are shown in § 4. Section 5 describes our wide-field search for an H I halo and for companions to WLM, and the possibility of a recent merger with a metal-poor H I cloud is discussed. The con-sequences of WLM possibly being a barred galaxy are con-sidered in § 6, and we summarize in § 7.

2. OBSERVATIONS AND DATA REDUCTION

WLM was observed with the Australia Telescope Compact Array (ATCA) in 1996 April and May. The observational

---

[1] Current address: Max-Planck-Institut für Astronomie, Königstuhl 17, D-69117 Heidelberg, Germany; cannon@mpia.de.

TABLE 1
BASIC PROPERTIES OF WLM

Quantity	Value	Reference
Right ascension, α (J2000.0)	00 01 57.8	1
Declination, δ (J2000.0)	$-15\ 27\ 51$	1
Heliocentric velocity, $V_\odot$ (km s^{-1})	-120 ± 4	2
	-130	3
Distance, D (Mpc)...	0.95 ± 0.04	4
Morphological type..	Ir IV-V	5
Total H I mass ($M_\odot$)	5.3×10^7	6
Full line width at half-power (km s^{-1})..........	20	7
Inclination angle (deg)...................................	69	8
Position angle (deg)..	181	2
Rotational velocity (km s^{-1}).........................	38	2
Conversion factor (pc arcmin^{-1})...................	276	2

NOTE.—Units of right ascension are hours, minutes, and seconds, and units of declination are degrees, arcminutes, and arcseconds.

REFERENCES.—(1) Gallouet et al. 1975; (2) de Vaucouleurs et al. 1991; (3) this work; (4) Dolphin 2000; (5) van den Bergh 1994; (6) Huchtmeier et al. 1981; (7) Huchtmeier & Richter 1986; (8) Ables & Ables 1977.

parameters and global H I data are listed in Table 2. A mosaic of seven pointings was done producing a $75' \times 75'$ field. The data were taken in the 375 and 750D configurations, with antenna six not in use in either, producing a synthesized beam size of $39'' \times 161''$ in right ascension and declination, respectively. The total on-source integration time was 27.25 hr. A bandwidth of 8 MHz divided into 1024 channels centered at -130 km s^{-1} yielded a velocity resolution of 1.65 km s^{-1}.

Calibration was done using the MIRIAD[2] software package. PKS 1934−638 and PKS 2354−117 were used as the primary and secondary flux, bandpass, and amplitude/phase calibrators, respectively. Velocities from -335 to -220 and from 40 to 70 km s^{-1} were chosen as representative of the continuum, and UVLIN was used to subtract the continuum emission from the spectral data. Fewer channels were used at lower frequency because contamination from Galactic H I became a problem at velocities above -40 km s^{-1}, as is shown in Figure 1.

Each pointing was cleaned separately using CLEAN and then combined with LINMOS to create the mosaic. This method proved better at removing sidelobes and other artifacts
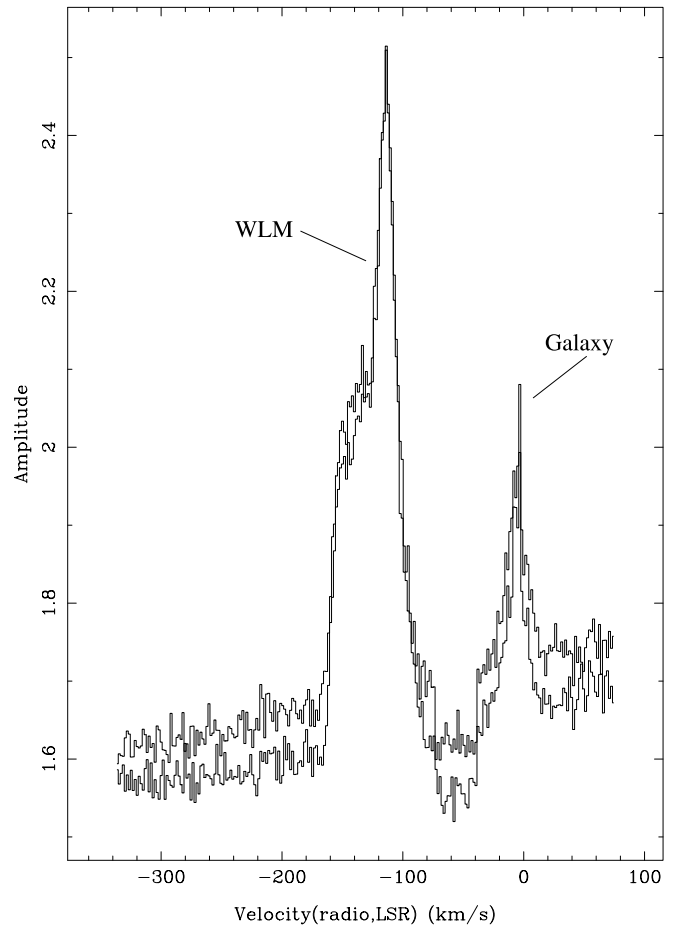
[2] See The MIRIAD User's Guide at http://www.atnf.csiro.au/computing/software/miriad.

FIG. 1.—Spectrum of WLM from data taken on 1996 April 12. Velocities from -335 to -220 and from 40 to 70 km s^{-1} were chosen to perform continuum subtraction, since they avoid contamination by Galactic H I. The upper and lower curves are for the yy and xx polarizations, respectively. See § 2.

than either MOSMEM or MOSSDI, which treat the full mosaic as a single datacube. A second datacube was created by smoothing the original cube with a Gaussian with full width at half-maximum (FWHM) of twice the beam width in right ascension and declination and a Hanning function with a width between first nulls of four channels in velocity. Any regions not containing flux 3 σ above the mean of a plane containing no real emission in the smoothed cube was blanked from the unsmoothed cube. The cube was then visually inspected, and

TABLE 2
ATCA H I OBSERVATIONS OF WLM

Quantity	Value
Dates of observations	1996 April 12, 13; May 21, 22, 23
Total bandwidth (MHz)......................................	8
Channel width (km s^{-1})....................................	1.65
Antenna baselines 375 Configuration (m)	31, 61, 92, 122, 184, 214, 245, 276, 337, 459
Antenna baselines 750D Configuration (m)........	31, 107, 184, 291, 398, 429, 582, 612, 689, 719
Synthesized beam FWHM (arcsec).....................	39×161
Conversion factor (K)[a]	95.59
Total H I flux (Jy km s^{-1})................................	149
Total H I mass ($M_\odot$)	$(3.2 \pm 0.3) \times 10^7$
Total dynamical mass ($M_\odot$)...............................	$(3.0 \pm 0.8) \times 10^8$

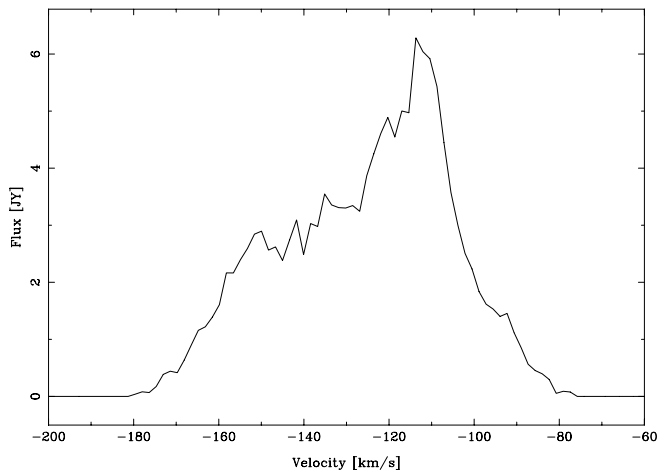[a] Equivalent to a 1 Jy beam^{-1} area.

FIG. 2.—High velocity resolution global H I emission profile of WLM. Note the strong asymmetry. This is discussed in more detail in § 4.

any signal not present in three consecutive planes was considered noise and blanked.

3. H I FLUX AND DISTRIBUTION OF WLM

3.1. *The Global* H I *Profile*

The global H I emission profile and channel maps are shown in Figures 2 and 3, respectively. We find a total integrated H I flux of 149 Jy km s^{-1}. Adopting a distance to WLM of 0.95 Mpc (Dolphin 2000) and using equation (1) of Roberts (1962) (see also the discussion by Giovanelli & Haynes 1988), the total H I mass is given by

$$M_{\rm H I} = 2.36 \times 10^5 \left(\frac{S_{\rm H I}}{\rm Jy\ km\ s^{-1}} \right) \left(\frac{D}{\rm Mpc} \right)^2 M_\odot, \qquad (1)$$

where $S_{\rm H I}$ is the source flux in units of Jy km s^{-1} and D is the distance in Mpc. We find a total H I mass of $(3.2 \pm 0.3) \times 10^7\ M_\odot$, which is smaller than the single-dish measurements of Huchtmeier et al. (1981) ($5.3 \times 10^7\ M_\odot$) and the recent Koribalski et al. (2004) value ($4.7 \times 10^7\ M_\odot$) from the HIPASS when corrected to the distance value adopted here. It is not surprising that we find a smaller value, since missing short-spacing information leaves us insensitive to large-scale emission, which is obvious since Huchtmeier et al. (1981) report an H I extent of 45′, which is 3 times the value we find. Note the asymmetric profile in Figure 2. Often such asymmetries are associated with interactions, and this presented additional motivation for a wide-field search for H I.

3.2. *The* H I *Distribution*

Figure 4 shows the total H I intensity map superposed on the stacked U image from the Local Group Survey of Massey et al. (2001). The distribution is relatively smooth at our resolution, and we are not resolving the structures left by supernovae and stellar winds that we would expect from a galaxy with a high current star formation rate (Dolphin 2000). H I emission can be seen to extend much past the optical body, which is typical of irregular galaxies; the H I exponential scale length of the major axis is 9′, compared to 3.′3 in the optical (Mateo 1998). Nearly elliptical isointensity contours are observed from the outermost regions of the galaxy to within

approximately 2′ in right ascension and 5′ in declination of the center, and the position angle of the major axis matches fairly well with that of the optical. In the northern half of the galaxy the H I emission follows the midplane of the galaxy with a slight concave warp toward the west. The stellar distribution in the north has a similar shape but with a much more pronounced warp; thus, the bulk of the H I emission in the north does not closely follow the stellar light distribution. In the southern half of the galaxy the H I flux is very well aligned with the stars out to the edge of the optical emission and then shifts slightly eastward.

Within 2′ in right ascension and 5′ in declination of the galaxy center, an offset double peak emerges. The origin of this double-peak structure is not obvious. It appears as though there are two separate systems with peaks that are offset by approximately 1′ in right ascension and 3′ in declination and with the westernmost of the two peaks at a radial velocity 20 km s^{-1} higher (more negative) than the eastern peak. This is reminiscent of the Sculptor Magellanic dwarf ESO 245-G005 (A143; Côté et al. 2000), which also has a multipeaked flux distribution with one of its peaks at an offset radial velocity from the rest of the galaxy. The implications of the double-peaked feature are discussed in § 5.

3.3. *Comparison with Optical Data*

Further inspection of the double-peak region shows additional new findings. Analysis of isophotes in B and V from Ables & Ables (1977) shows what could be patchy regions of extinction that subtend much of the southern part of WLM. An analysis of U, B, and V images from the Local Group Survey (Massey et al. 2001) identifies regions of higher values of both $U-B$ and $B-V$ in the southern part of the galaxy (relative to regions in the north; see Fig. 5). These regions are found in fingers that run between H II regions from the outer to the inner galaxy. Of the two peaks in emission we observe, the eastern one is roughly aligned with one of these extinction regions, while the western peak lies just north of a large complex of H II regions. The all-sky Galactic extinction map produced by Schlegel et al. (1998) shows $E(B-V)$ at levels of only 0.02–0.03 mag; thus, we assume this extinction to be internal to WLM (although the Schlegel et al. observations do not resolve the galaxy, so we cannot be sure from their maps that there is no small-scale Galactic extinction). Additionally, the H II regions mapped by Hodge & Miller (1995) all lie either adjacent to or along the line of sight to these extinction regions. A possible explanation of this extinction is the presence of a large molecular gas complex in the southern half of WLM. The only search for any type of molecular gas was that of Taylor & Klein (2001). Their CO observations resulted in a nondetection; however, they point out that in low-metallicity systems like WLM, there is evidence for a high CO-to-H$_2$ conversion factor (Taylor et al. 1998). Also, their beam size was small enough that they were only able to observe a relatively small fraction of the galaxy, with those observations focusing on parts of the galaxy near the H II regions observed by Hodge & Miller (1995). Since CO had been found near H II regions in other Local Group dwarf irregular galaxies, this was an excellent place to begin their search; however, these regions, in large part, do not coincide with the regions we find to have the highest extinction. Thus, it is still possible to have a substantial amount of molecular hydrogen in the galaxy without any CO detected. We also inspected radio continuum maps to search
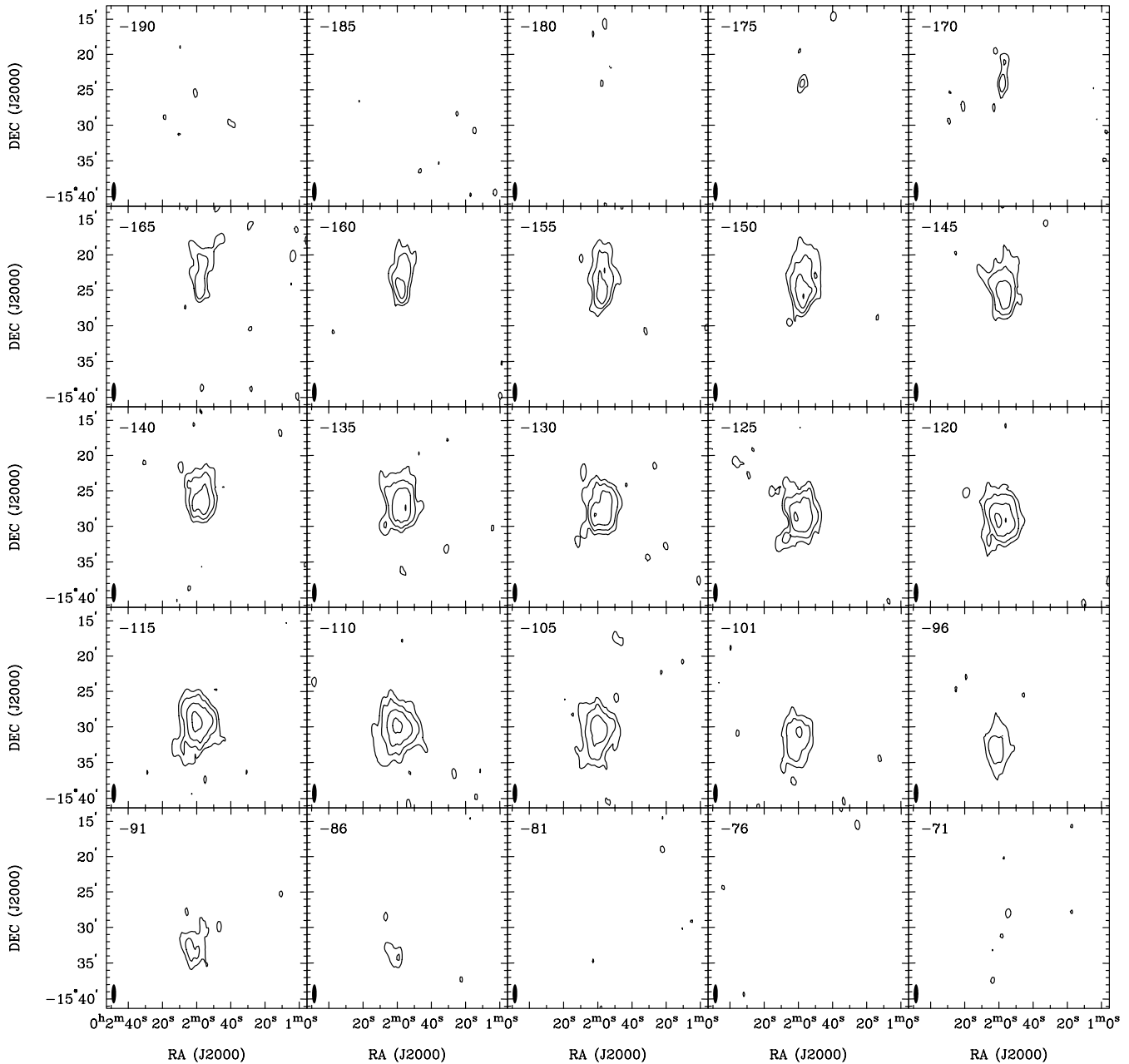
FIG. 3.—Channel maps for WLM. Contours are 2.5, 5, 10, and 20 σ above the mean of the background ($\sigma = 18$ mJy beam^{-1}). The synthesized beam size is shown (*filled ellipse*) in the lower left corner.

for emission from embedded super star clusters, which we might expect to observe since WLM is a late-type star-forming galaxy, but none were detected.

4. H I POSITION-VELOCITY DIAGRAMS AND THE ROTATION CURVE

Except in the far northern and southern parts of the galaxy, the isovelocity contours of WLM (shown overlaid on the total H I intensity map in Fig. 6) are relatively parallel, which is consistent with regular solid-body rotation. In the far north and south the contours take on the characteristic shape of differential rotation, showing where the rotation curve begins to flatten. Overall, the velocity field is fairly symmetric, with some deviations we are unable to resolve along the southeastern edge of the galaxy. This largely symmetric velocity distribution with slight departures is typical of dwarf irregular

galaxies (Skillman 1996). One noticeable asymmetry is the offset in velocity between the western and eastern sides of the galaxy. Although the major axis of the galaxy has a nearly north-south orientation, the isovelocity contours do not align with constant declination and show a difference of roughly 10 km s^{-1} from one side of the galaxy to the other.

In Figure 7 we show position-velocity diagrams for slices running from north to south through the east emission peak, the nominal galaxy center, and the west emission peak, respectively. Like the H I flux distribution, the position-velocity diagrams describe a mostly uniform rotating disk galaxy, with some subtleties. First, the H I emission from the eastern slice is offset from that of the western slice by approximately 20 km s^{-1}. Second, the eastern slice shows a bifurcation in H I velocity near the center of the galaxy. This can also be seen in the central and western slices but is most prominent in the east.
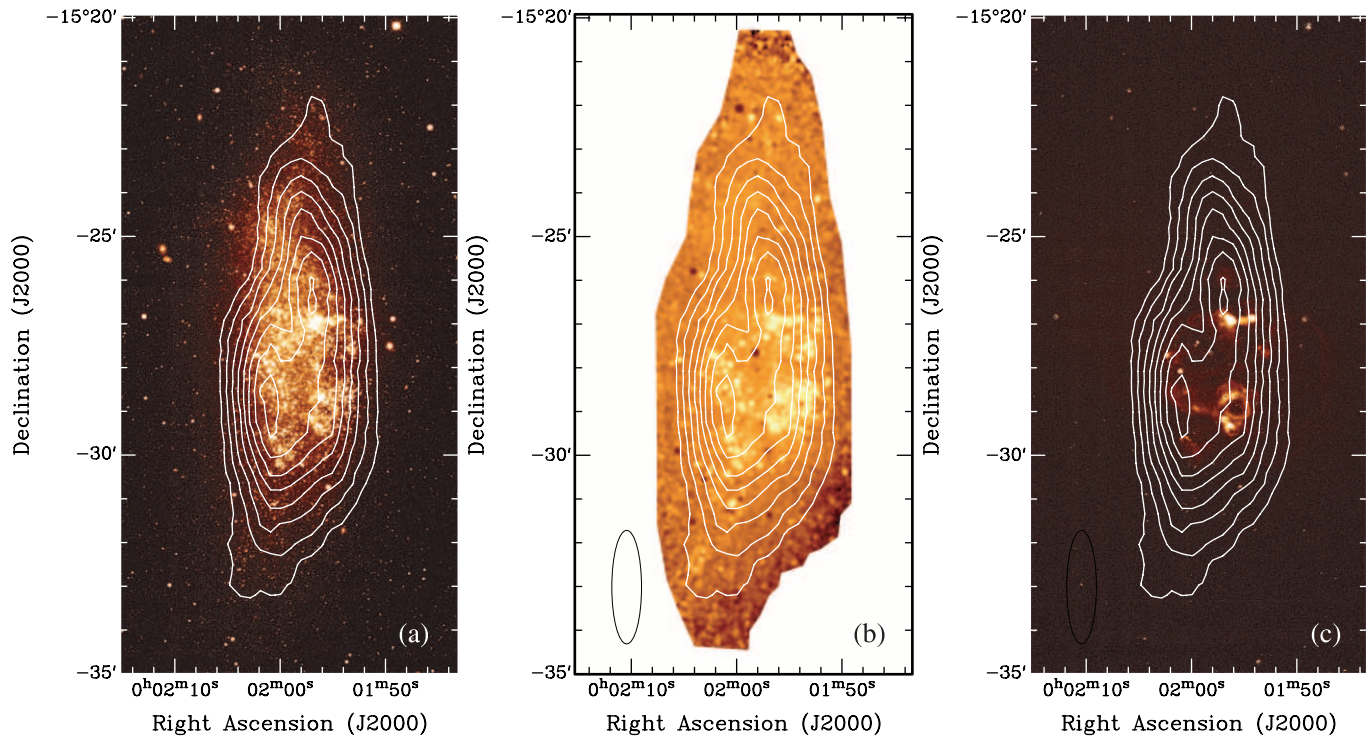
FIG. 4.—(a) Total H I intensity map of WLM superposed on the Local Group Survey U image (Massey et al. 2001). Contours are from 25% to 95% of the peak column density (2.16×10^{21} cm^{-2}) in increments of 10%. (b) Same H I contours superposed on the $U-B$ image. The image has been blanked against the first moment map to remove low–signal-to-noise data. The synthesized beam size for the H I data is shown in the lower left corner. (c) Continuum-subtracted Hα image from the Local Group Survey, again with our H I contours superposed. Note the two H I peaks and their relationship to the bright stellar clusters and H II regions.

Because of our relatively poor resolution in declination, it is not clear what role beam smearing is playing in our perception of this feature; it could be due to a single H I cloud at a discrepant velocity, or it could really be an extended feature as it appears in Figure 7. This structure may be indicative of a bar in WLM and is discussed further in § 6.

It is also possible that a gaseous blowout created by a stellar association is responsible for displacing gas northeast of the galaxy center and creating the multicomponent position-velocity diagrams. Holes are relatively common in the disks of dwarf irregular galaxies (Skillman 1996), and sometimes they are directly associated with H I at discrepant velocities indicative of blowout (e.g., IC 10 [Shostak & Skillman 1989; Wilcots & Miller 1998]; NGC 1569 [Israel & van Driel 1990; Stil & Israel 2002]; Ho II [Puche et al. 1992]). For a disk seen edge-on, it may not be possible to see the holes, and the only evidence of blowout would be gas at discrepant velocities (e.g., NGC 625; Cannon et al. 2004). However, no Hα is observed in this region, and there is no evidence of a young stellar association or cluster. Thus, if a blowout did occur, it would have to be a relatively old feature (>10–20 Myr). Additionally, the offset between the velocities seen in the western and eastern parts of the galaxy is continuous over most of the disk, so a localized blowout event seems an unlikely explanation for the offset. Ultimately, higher resolution and higher sensitivity H I observations and deeper optical imaging should be able to determine the nature of the discrepant velocity of H I.

Rotation curves (see Fig. 8) were created by fitting a tilted-ring model (Begeman 1987) to the velocity field shown in Figure 6. The velocity field was divided into concentric rings, each 162″ in width, and six parameters (systemic velocity, rotational velocity, position angle, inclination, and x and y kinematical centers) were iteratively fitted to best model the observed radial velocity. Rotation curves were created using only the approaching half of the galaxy, only the receding half of the galaxy, and the entire galaxy. The systemic velocity and galaxy center were determined first, beginning with values from the global profile and optical data, respectively, then fixed for all rings. The inclination was fitted to the optical value of 69° because it was not well constrained by the H I data. The position angle was allowed to vary, yet on both sides of the galaxy it only changed by approximately 4°.

For the final rotation curve the position angle was fixed at 181°, which was the average value when allowed to vary, leaving the rotational velocity as the only parameter free to vary. Errors were determined by adopting the larger of either the formal errors from the fits or the difference between the velocity with the position angle fixed and the velocity with the position angle free. A significant limitation to our rotation curve analysis was that our beam was elongated in the same direction as the galaxy, leaving us few data points for the final rotation curves. Because of this, we do not attempt a detailed mass modeling of the galaxy, instead leaving that task for higher resolution studies.

The morphology of the rotation curves are typical of a disk system, showing solid-body rotation in the inner galaxy and differential rotation in the outer. For the total dynamical mass determination we adopt the last measured data point (38 ± 5.0 km s^{-1} at 0.89 kpc) from the rotation curve using the entire galaxy. This maximum velocity is typical of galaxies with similar absolute B magnitudes (Côté et al. 2000). Assuming a spherically symmetric dark matter distribution, this yields a total dynamical mass of $(3.00 \pm 0.80) \times 10^{8}\ M_{\odot}$. The
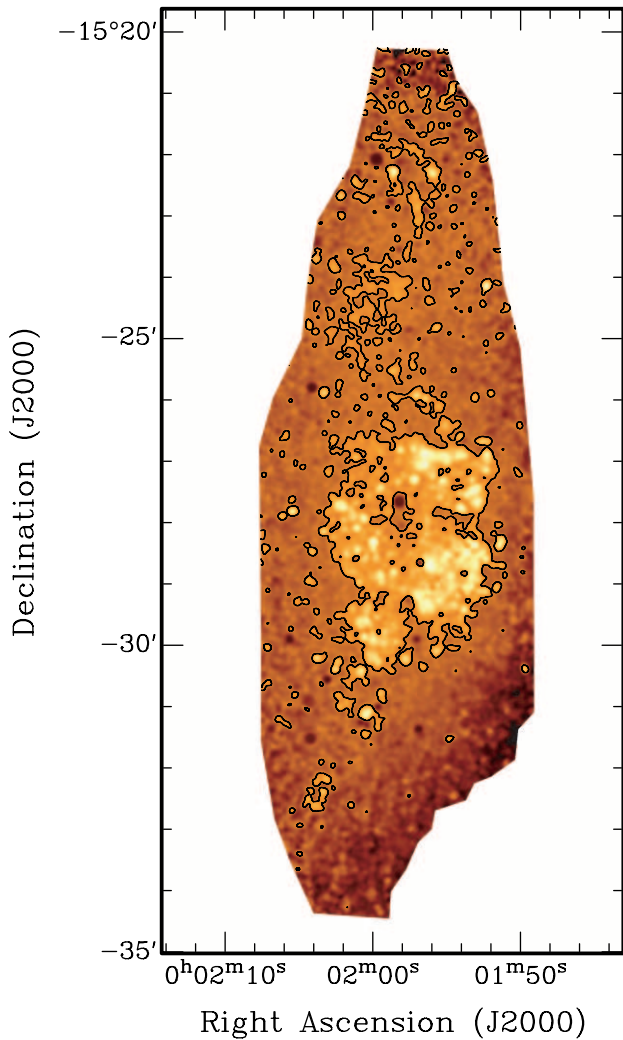
Fig. 5.—A $U-B$ image using data from Massey et al. (2001). A contour is added to guide the reader's eye to redder (darker) regions in the central part of the galaxy. These regions are likely due to extinction internal to WLM associated with molecular gas. See § 3.3.

Fig. 6.—Total intensity map for WLM with the velocity field overlaid. Contours range from -155 km s^{-1} (top) to -100 km s^{-1} (bottom) in increments of 5 km s^{-1}. The three lines at top and bottom show which cuts were used to create the position-velocity diagrams in Fig. 7. Note the systematic shift in velocity from the east to the west.

$(M/L_B)_{dyn}$ value at the last measured point is 5.9, which is also typical of dwarf irregular galaxies at this radius. It should again be noted, however, that because of our lack of sensitivity to large-scale structures, we are missing a significant amount of H I at large radii and thus are certainly not measuring the entire dynamical mass of the galaxy.

5. WIDE-FIELD SEARCH FOR H I

After Minniti & Zijlstra (1996) suggested the existence of an extended stellar halo in WLM, mosaic imaging was proposed to search for an associated H I halo. This search took on greater importance after a recent study by Venn et al. (2003) found a supergiant with an oxygen abundance 0.68 dex (>3 σ) higher than the nebular abundance from sampled H II regions (Hodge & Miller 1995). This is a serious problem, since stars form out of and thus should not have higher abundances than the nearby ISM, so the possibility existed that this could be the signature of a recent merger with a low-metallicity H I cloud. It is interesting to note that ESO 245-G005, which has a multicomponent flux distribution and velocity field, like WLM, was found by Miller (1996) to have a strong abundance gradient along its bar, which is not typical of this type of
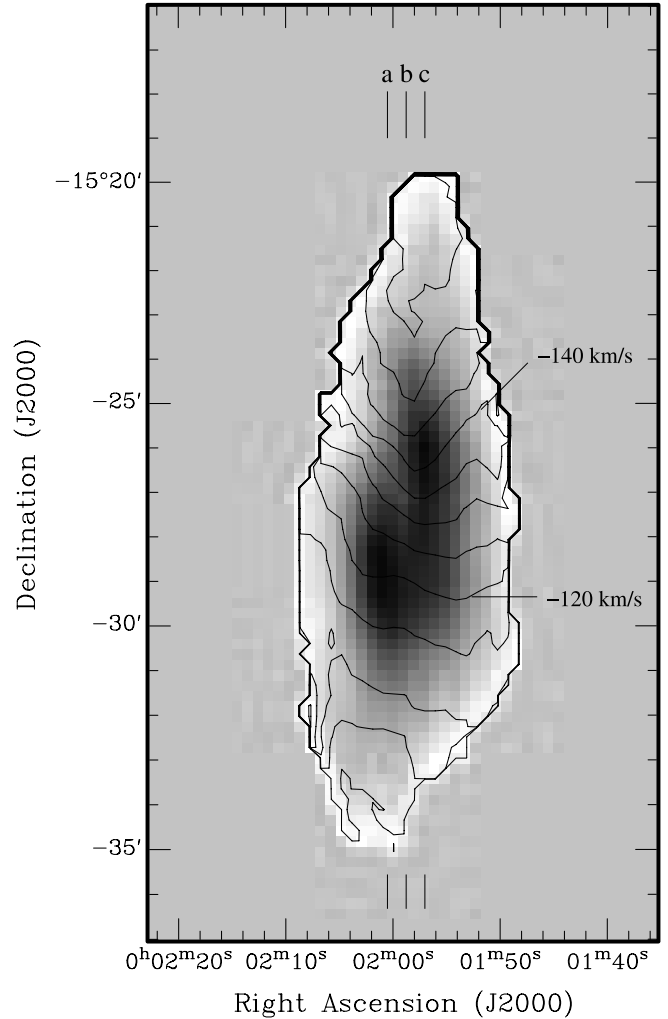
galaxy. Côté et al. (2000) postulate that this could be due to the accretion of an H I cloud of different metallicity or that the entire galaxy is the result of a recent merger that has not yet been able to completely mix its metals. Their argument is strengthened by the observations of Miller (1996), Taylor et al. (1995), and others who have found that a large fraction of irregular and H II galaxies have H I companions. Additionally, WLM's H I global profile shows strong asymmetry, which is often associated with interactions in spiral galaxies.

Venn et al. (2003) were skeptical that the accretion of an H I cloud could be responsible for the abundance anomaly, because within the last 10 Myr (the lifetime of a supergiant) a cloud more massive than 10^6 $M_\odot$ would had to have been accreted to dilute the ISM sufficiently to produce the observed abundances. Because the overall H I distribution is smooth and the rotation curves for the approaching and receding portions of the galaxy are nearly identical, with no tidal structures observed, we see no compelling kinematic evidence of a recent interaction or merger. Additionally, we created a cube with 3 times lower resolution than the full-resolution cube to search for extended low surface brightness features like we might expect from a low-mass companion. A plane-by-plane search revealed no such companions to a 3 σ mass limit of
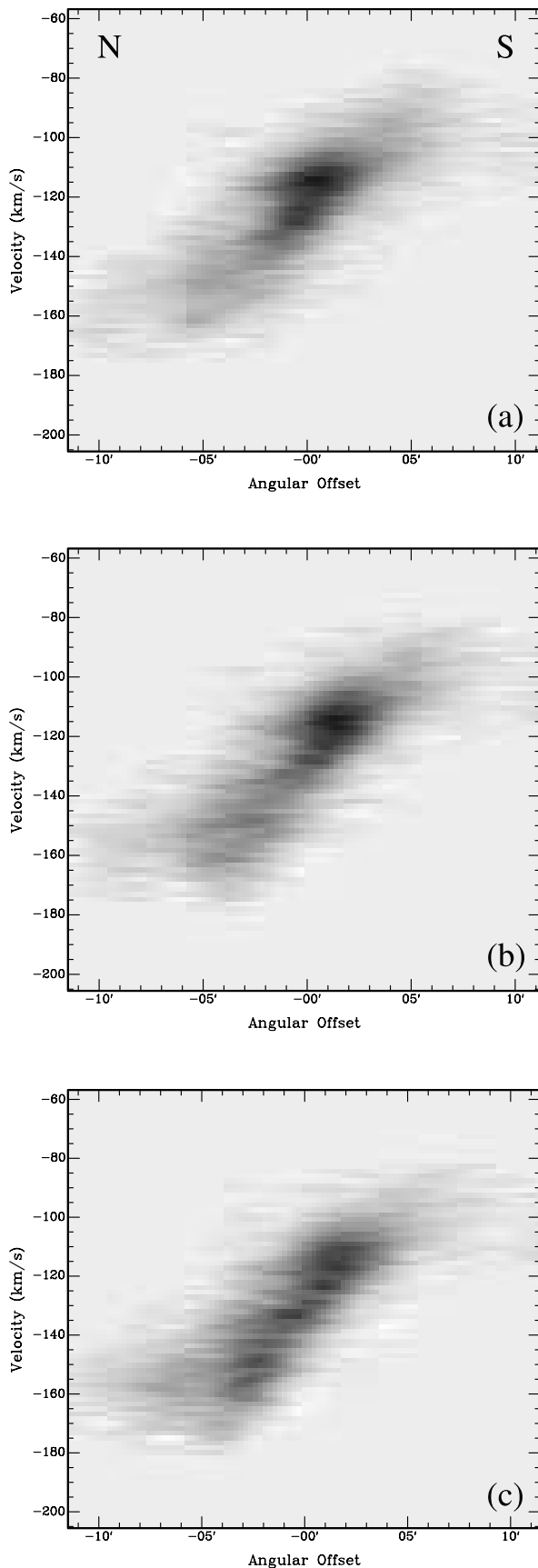
FIG. 7.—Position-velocity diagrams for cuts running north to south through (a) the easternmost of the two emission peaks, (b) the nominal galaxy center, and (c) the westernmost emission peak. There appears to be a two-component nature, which we discuss in § 4.
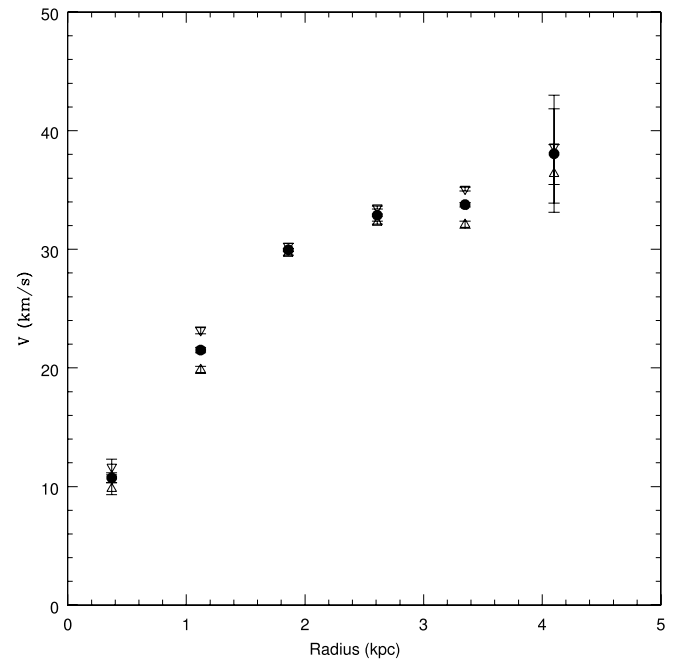

FIG. 8.—Rotation curves for WLM. Upward-pointing triangles are for the rotation curve created using only the receding (south) side of the galaxy, downward-pointing triangles are for only the approaching (north) side of the galaxy, and filled circles are for the full galaxy. All rotation curves were done with fixed systemic velocity of -127 km s^{-1}, position angle of $181°$, and inclination angle of $69°$. Note the good agreement between the independent measurements from the two sides of the galaxy and the transition from solid-body to differential rotation at approximately 2 kpc.

8.4×10^5 $M_\odot$ (assuming a velocity width of 15 km s^{-1}), although because WLM is a bright source resolved by our beam we were unable to completely remove the first sidelobe, whose peak lies approximately 7.'5 east and west of the galaxy center. This leaves us less sensitive to any companions that may exist in this region. Finally, Minniti & Zijlstra (1996) postulated the existence of a stellar halo from deep V and I photometry. Their data showed the red stars to be less centrally distributed than the blue stars and attributed the difference in stellar population between the inner and outer part to a flattened Population II halo extending to 2 kpc from the galaxy center. More recently, however, Battinelli & Demers (2004) performed a survey of C stars in WLM and found no evidence to support the Minniti & Zijlstra (1996) conclusion. In this investigation we see no evidence of any extended H i emission that would be consistent with a gaseous halo.

6. IS WLM A BARRED GALAXY?

Perhaps a better explanation for the somewhat peculiar flux distribution and irregular structure in the position-velocity diagrams is the presence of a bar. Simulations of gas dynamics in barred spiral galaxies (Roberts et al. 1979) have shown that a bar and its associated shocks are capable of depleting gas from the inner parts of the galaxy and piling it up near where the end of the bar meets the spiral arms. This is borne out in observations of many barred galaxies with giant H ii regions found at the ends of their bars. This is particularly true of Magellanic irregular galaxies. Elmegreen & Elmegreen (1980) found that 30%–50% of barred irregular galaxies in their sample had large peripheral H ii regions and that these regions are usually near one end of the bar. Interestingly, WLM's largest H ii region appears near the southwest edge of the

stellar distribution. However, whether this region is actually at the periphery of the galaxy and furthermore whether or not WLM is a barred system may be impossible to determine because of its high inclination angle (69°). However, if a bar does exist, it might be capable of displacing enough gas to produce a multipeaked flux distribution, as well as inducing noncircular motions in the gas to create the observed peculiarities in the position-velocity diagrams. This hypothesis does not explain the abundance anomaly, but again, more spectroscopic observations are needed to resolve this question.

7. RESULTS AND CONCLUSIONS

We have presented ATCA neutral hydrogen mosaic imaging of the dwarf irregular galaxy WLM. We find a total H I flux of 149 Jy km s^{-1} and, adopting a distance of 0.95 ± 0.04 Mpc, a total H I mass of $(3.2 \pm 0.3) \times 10^7\ M_\odot$. This mass is significantly lower than the single-dish measurement of Huchtmeier et al. (1981), which is expected since we are insensitive to large-scale emission due to short-spacing information.

At our resolution the H I distribution is smooth and extends past the optical distribution by a factor of approximately 3, which is typical of this type of galaxy. In the northern half of the galaxy the H I exhibits a slight warp toward the west, although it is not as pronounced as that of the stars, so the bulk of the H I does not closely trace the stellar light distribution. In the southern half of the galaxy the H I is aligned with the stars out to the edge of the optical emission then shifts somewhat eastward. In the center of WLM we detect a double-peaked core not previously resolved. The peaks are separated by approximately 1′ in right ascension and 3′ in declination, with the northern peak at a radial velocity 20 km s^{-1} higher than the southern, and while the northern peak is smooth in position-velocity space, the southern peak is confined to between -110 and -130 km s^{-1}. The stellar halo proposed by Minniti & Zijlstra (1996) led us to conduct a wide-field search, 38′ in radius, for an associated gaseous halo, but we observe the H I to fall smoothly into the background and thus see no evidence for such a halo in H I.

Inspection of the central core of WLM from a previous optical study (Ables & Ables 1977), as well as our own analysis of recently released data (Massey et al. 2001), shows what appear to be regions of significant extinction in the southern half of the galaxy. Because the Galactic extinction maps of Schlegel et al. (1998) show very little extinction along this line of sight and because we find variable extinction values within

the galaxy, we conclude that the extinction is internal to WLM and produced by a complex of molecular clouds that are outlined by previously mapped H II regions (Hodge & Miller 1995).

The isovelocity contours of WLM are nearly parallel over most of the galaxy, which is consistent with solid-body rotation. In the far north and south the contours take on the characteristic shape of differential rotation, showing where the rotation curve flattens. The velocity field is mostly symmetric, with some deviation along the southeastern edge of the galaxy that we are unable to resolve.

We do know that WLM has a double-peaked flux distribution. We also see some irregularity in the position-velocity diagrams that, when combined with the abundance anomaly of Venn et al. (2003), present an interesting puzzle, since we see no kinematic evidence of a recent merger. One possible explanation for these observations is that WLM is a barred galaxy. Bars in dwarf irregular galaxies have been observed to deplete gas from the inner parts of the galaxy and deposit it near the ends of the bar. Typically, giant H II regions are found near where the bar meets the spiral arm. This would explain both the unusual flux distribution and velocity structures; however, WLM's high inclination may make this determination impossible. Only higher resolution studies of WLM will be able to shed light on what the true cause of the multipeaked core is and if WLM does have a multicomponent velocity field.

REFERENCES

Ables, H. D., & Ables, P. G. 1977, ApJS, 34, 245
Battinelli, P., & Demers, S. 2004, A&A, 416, 111
Begeman, K. 1987, Ph.D. thesis, Univ. Groningen
Cannon, J. M., McClure-Griffiths, N. M., Skillman, E. D., & Côté, S. 2004, AJ, 607, 274
Côté, S., Carignan, C., & Freeman, K. C. 2000, AJ, 120, 3027
de Vaucouleurs, G., de Vaucouleurs, A., Corwin, H. G., Jr., Buta, R. J., Paturel, G., & Fouqué, P. 1991, Third Reference Catalogue of Bright Galaxies (New York: Springer)
Dolphin, A. E. 2000, ApJ, 531, 804
Elmegreen, D. M., & Elmegreen, B. G. 1980, AJ, 85, 1325
Gallouet, L., Heidmann, N., & Dampierre, F. 1975, A&AS, 19, 1
Giovanelli, R., & Haynes, M. P. 1988, in Galactic and Extragalactic Radio Astronomy, ed. G. L. Verschur & K. I. Kellermann (Berlin: Springer), 522
Hodge, P., & Miller, B. W. 1995, ApJ, 451, 176
Huchtmeier, W. K., & Richter, O. G. 1986, A&AS, 63, 323
Huchtmeier, W. K., Seiradakis, J. H., & Materne, J. 1981, A&A, 102, 134

Israel, F. P., & van Driel, W. 1990, A&A, 236, 323
Koribalski, B. S., et al. 2004, AJ, 128, 16
Massey, P., Hodge, P. W., Holmes, S., Jacoby, G., King, N. L., Olsen, K., Saha, A., & Smith, C. 2001, BAAS, 33, 1496
Mateo, M. 1998, ARA&A, 36, 435
Melisse, J. P. M., & Israel, F. P. 1994, A&AS, 103, 391
Melotte, P. J. 1926, MNRAS, 86, 636
Miller, B. 1996, AJ, 112, 991
Minniti, D., & Zijlstra, A. A. 1996, ApJ, 467, L13
Puche, D., Westpfahl, D., Brinks, E., & Roy, J. 1992, AJ, 103, 1841
Roberts, M. S. 1962, AJ, 67, 431
Roberts, W. W., Huntley, J. M., & van Albada, G. D. 1979, ApJ, 233, 67
Schlegel, D. J., Finkbeiner, D. P., & Davis, M. 1998, ApJ, 500, 525
Shostak, G. S., & Skillman, E. D. 1989, A&A, 214, 33
Skillman, E. D. 1996, in ASP Conf. Ser. 106, The Minnesota Lectures on Extragalactic Neutral Hydrogen, ed. E. D. Skillman (San Francisco: ASP), 208

Stil, J. M., & Israel, F. P. 2002, A&A, 392, 473
Taylor, C. L., Brinks, E., Grashuis, R. M., & Skillman, E. D. 1995, ApJS, 99, 427
Taylor, C. L., & Klein, U. 2001, A&A, 366, 811
Taylor, C. L., Kobulnicky, H. A., & Skillman, E. D. 1998, AJ, 116, 2746
van den Bergh, S. 1994, AJ, 107, 1328
———. 2000, The Galaxies of the Local Group (Cambridge: Cambridge Univ. Press)

Venn, K. A., Tolstoy, E., Kaufer, A., Skillman, E. D., Clarkson, S. M., Smartt, S. J., Lennon, D. J., & Kudritzki, R. P. 2003, AJ, 126, 1326
Wilcots, E. M., & Miller, B. W. 1998, AJ, 116, 2363
Wolf, M. 1910, Astron. Nachr., 183, 187